Hindawi
Mathematical Problems in Engineering
Volume 2019, Article ID 9134952, 11 pages
https://doi.org/10.1155/2019/9134952

Research Article

Fault-Tolerant Supervisory Control for Dynamic Positioning of Ships

Xiaogong Lin, Heng Li, Kun Liang, Jun Nie, and Juan Li

College of Automation, Harbin Engineering University, Harbin 150001, China

Correspondence should be addressed to Heng Li; wsqess@foxmail.com

Received 6 August 2018; Accepted 17 December 2018; Published 3 January 2019

Academic Editor: A. M. Bastos Pereira

A fault-tolerant supervisory control method for dynamic positioning of ships with actuator failures and sensor failures is presented in this paper. Unlike the traditional fault detection and control, fault detection and fault-tolerant controller are designed as a unit in this paper through a supervisor. By introducing a nonlinear estimation error and virtual controller, the sensor failures are separated from the actuator failures in the supervisory control system. It guarantees that the detectability property and matching property of the switched system are satisfied. Firstly, a new extended state observer is designed to match the models of different actuator failures. Secondly, by introducing a virtual controller, the detectability property of the switched system is guaranteed. Finally, a nonlinear estimation error operator is used in the designing of switching logic to guarantee stability of the closed-loop system with sensor failures. When sensor failures and actuator failures occur, we show that all the states of the closed-loop system are guaranteed to be bounded. The effectiveness of the fault-tolerant control is verified by simulation experiments.

1. Introduction

It is well known that failures can lead to a significant degradation in the performance of plant and may even make the system unstable. These considerations provide a strong motivation for the pursuit of systematic strategies for the designing of fault-tolerant controller (FTC) that ensure the stability of the system in case of failures and reduce the risk of safety hazards. FTC has attracted much attention in control community in the last two decades, and several methods can be found in the literatures [1–5].

Dynamic positioning system (DPS) can only rely on its own propulsion to counteract the interference of the external environment [6, 7]. Since the highly disturbed marine environment will lead to aging of the components, which causes inevitable malfunctions in actuators, measurement sensors and process equipment. Therefore, how to design a fault-tolerant controller for DPS is a critical problem. The challenges to be met when designing FTC for DPS are complex dynamic behavior due to strong nonlinearities, model uncertainty, and environmental force, which makes fault process difficult to monitor and control [8–10].

Over the last decade, some research on FTC for DPS has been carried out. Fu and Ning proposed a method for online control reconfiguration of FTC to dynamic positioning vessel using disturbance decoupling methods [11]. Andrea and Tor utilized an unknown input observer technique to produce a fault detection and isolation (FDI) mechanism for an overactuated marine vessel [5]. Fault detection and diagnosis mechanism, based on two techniques: the parity space approach and the Luenberger observer, was proposed to guarantee a fault-tolerant robust control for the dynamic positioning of an overactuated offshore supply vessel [12]. Du et al. constructed an iterative learning observer to estimate the fault signal and combined the pseudoinverse method to generate a fault-tolerant controller for the dynamic positioning system [13]. Other remarkable results on FTC for dynamic positioning vessels can be found in [14–16]. So far, most of FTC methods for DPS are based on the low-frequency model of the ship and also generally assume that the upper bound of external disturbances is known, which is often difficult

to determine in practice. Moreover, the traditional FTC is based on the FDI mechanism which will reduce the real-time performance of the controller when the system is complex enough.

Motivated by the above considerations, a fault-tolerant supervisory control method for dynamic positioning of ships with actuator failures and sensor failures is presented in this paper. We consider the possible faults as the uncertainty of the system and use the supervised switching mechanism instead of the traditional fault detection and diagnosis mechanism to achieve fault-tolerant control in this paper. When faults occur, the dynamic characteristics of the controlled system will change abruptly, so the controller can be quickly adapted through the discontinuous changing switching signal. The novelty of the approach with respect to existing results consists of the following key-points:

(1) Unlike in [11, 13, 15] where FTC methods for DPS are only based on the low-frequency model of the vessel which limits the range of applicability. To this end, in this paper, FTC method for dynamic positioning vessel with wave-frequency model is introduced.

(2) In [13, 14], the authors made restrictive assumptions on the external disturbance, for example, the upper bound of disturbances is known. Instead, in the proposed work, such restrictive assumption is not needed.

(3) Unlike in [5] where FDI mechanism is needed, in this paper, FDI mechanism is not needed due to the introduction of injected system and supervisor. Besides, the number of fault actuators in [5] is affected by the structure of actuator matrix, while not in this paper.

The remainder of this paper is organized as follows. In Section 2, the model of ships is introduced and the structure of supervisory fault-tolerant control system is formulated. Section 3.1 presents a method to design multiestimator for dynamic positioning vessel based on wave-frequency model. A candidate controller for each estimator is proposed in Section 3.2. In Section 3.3 a nonlinear estimation error operator is proposed for sensor failures. The fault-tolerant supervisory control system is presented in Section 3.4. In Section 4, we illustrate the effectiveness of the proposed method via simulations on the DP vessel. Finally, some concluding remarks are included in Section 5.

2. Preliminaries

2.1. Modeling of Ships. For the horizontal motion of a surface vessel, let the earth-fixed position (x, y) and the orientation ψ of the vessel relative to an earth-fixed frame $X_E Y_E Z_E$ be expressed in vector form by $\eta = [x, y, \psi]^T$, and let the velocities decomposed in a body-fixed reference frame XYZ be represented by the state vector $\nu = [u, v, r]^T$. These three modes are referred to as the surge, sway, and yaw of a vessel [6, 17]. The origin of the body-fixed reference frame XYZ is located at the vessel center line in a distance x_G from the center of gravity, as shown in Figure 1.

The transformation between the body-fixed velocity and the earth-fixed velocity vectors can be written as

$$\dot{\eta} = J(\eta)\nu \tag{1}$$

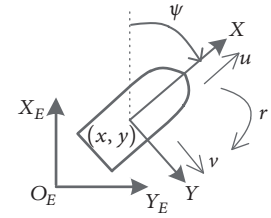

Figure 1: Vessel Reference Frames.

where $J(\eta)$ is a rotation matrix. In the remainder of the paper, the rotation matrix in yaw is defined as

$$J(\eta) = J(\psi) = \begin{bmatrix} \cos\psi & -\sin\psi & 0 \\ \sin\psi & \cos\psi & 0 \\ 0 & 0 & 1 \end{bmatrix} \tag{2}$$

In the mathematical modeling of ship dynamics, it is common to separate the model into a low-frequency model and wave-frequency model. The wave-frequency motion of the ship is due to 1st-order wave loads. The low-frequency motion is driven by 2nd-order mean and slowly-varying wave, current, wind, and thrust forces and the restoring forces from the mooring system [6, 18]. The total motion of the ship is given as the sum of the low-frequency and the wave-frequency contributions:

$$\begin{aligned} \dot{\xi} &= A_W \xi + B_W \omega_w \\ \dot{\eta} &= J(\psi)\nu \\ \dot{b} &= -A_b^{-1} b + B_b \omega_b \\ M\dot{\nu} &= TKT_p + J^T(\psi) b - D\nu, \quad K \in \aleph \\ y &= \eta + \eta_w + \omega_y \end{aligned} \tag{3}$$

where $\xi \in \mathbb{R}^6$ is the wave state vector and $A_W \in \mathbb{R}^{6\times 6}, B_W \in \mathbb{R}^{6\times 3}$ are matrices related to the wave peak frequency $\omega_{0i}, i = \{1, 2, 3\}$, and relative damping ratio $\zeta_i, i = \{1, 2, 3\}$. $\eta_w = C_W \xi \in \mathbb{R}^3$ is the wave frequency motion vector in the earth-fixed frame, and $C_W \in \mathbb{R}^{3\times 6}$ is wave frequency measurement matrix. $b \in \mathbb{R}^3$ is a bias term representing slowly varying environmental forces and moment, and $A_b \in \mathbb{R}^{3\times 3}, B_b \in \mathbb{R}^{3\times 3}$ are the diagonal matrix of positive bias time constants and diagonal matrix scaling the amplitude of ω_b, respectively. $\omega_w \in \mathbb{R}^3, \omega_b \in \mathbb{R}^3, \omega_y \in \mathbb{R}^3$ are vectors of zero-mean Gaussian white noise. $M \in \mathbb{R}^{3\times 3}$ is the inertia matrix including hydrodynamic added inertia and $D \in \mathbb{R}^{3\times 3}$ is the damping matrix. $T \in \mathbb{R}^{3\times m}, K \in \mathbb{R}^{m\times m}$, and $T_p \in \mathbb{R}^m$ are thruster structure matrix, coefficient matrix, and thrust force vector, respectively. $\aleph$ denotes all possible actuator failures. For more details, please refer to the literature [6, 19].

2.2. Supervisory Control. Supervisory control has attracted significant research efforts and various approaches have been developed. Supervisory control used for uncertain system is

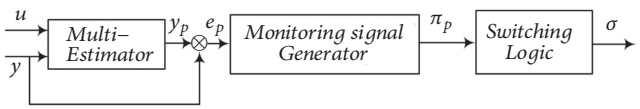

FIGURE 2: Supervisor Architecture.

more advantageous than gain scheduling control in terms of flexibility and modularity. In supervisory control, one builds a bank of alternative candidate controllers and switches among them based on measurements collected online. The switching is orchestrated by a specially designed logic that uses the measurements to assess the performance of the candidate controller currently in use and also the potential performance of alternative controllers. The need for switching arises from the fact that no single candidate controller would be capable, by itself, of guaranteeing good performance when connected with the uncertain process [20–25].

In supervisory control system, the controller selection is carried out by a high-level supervisor. The supervisor is a hybrid system with continuous states and discrete states. The behavior of the process is compared with the behavior of a several admissible process models by the supervisor to determine which model is more likely to describe the actual process. Then the candidate controller that is more adequate for the estimated model is placed in the loop [20, 22, 25]. The supervisor comprises three subsystems: multiestimator, monitoring signal generator, and switching logic (see Figure 2), where u, y are input and output of the process, $e_p(p \in P)$ is the estimation error, $\pi_p(p \in P)$ is monitoring signal which is suitable function of the estimation error, and σ is the control switching signal. There are four important properties of supervisory control systems, which are matching property (M.P), detectability property (D.P), nondestabilization property (N.P), and small error property (S.P) [22, 26].

(i) M.P: The multiestimator should be designed such that at least one of the estimation errors converges to zero exponentially fast.

(ii) D.P: For every fixed estimator/observer, the total switched system must be detectable with respect to the corresponding estimation error e_p, when the control switching signal σ is frozen at $\sigma = \chi(p)$, where χ is controller selection function.

(iii) S.P: The S.P calls for a bound on e_ρ in terms of the smallest of the signals $e_p, p \in P$ for a process switching signal ρ for which $\sigma = \chi(\rho)$.

(iv) N.P: The control switching signal σ is said to have the N.P if it preserves the detectability in a time-varying sense; i.e., the switched system is detectable with respect to the switched output e_ρ, for a process switching signal ρ for which $\sigma = \chi(\rho)$.

The stability of the supervisory control system can be guaranteed when the four properties above are satisfied [27].

2.3. Assumptions and Lemmas. Throughout this paper, the following assumptions are made.

Assumption 1. For low speed applications it can also be assumed that $M^T = M > 0$ and $D = D^T > 0$.

Remark 2. Assumption 1 is true if starboard and port symmetries and low speed are assumed [28].

Assumption 3. In the Lyapunov stability analysis of the observer, some fair assumptions are made: $\omega_b = \omega_y = \omega_w = 0$, and $J(\psi) = J(\psi + \psi_W)$.

Remark 4. The bias and wave models are driven by zero-mean Gaussian white noise. These terms are omitted in the observer model and Lyapunov stability analysis since the estimator states are driven by the estimation error instead. Besides, zero-mean Gaussian white measurement noise is negligible compared to the wave disturbances η_w [29].

Assumption 5. The acceleration vector is available for measurement.

Remark 6. Recently high performance inertial measurement units (IMU) are becoming increasingly affordable and integrated navigation systems (INS) that integrate IMU and GPS reproduce not only positions but also accelerations with great accuracy to a reasonable price. So it is possible to adopt acceleration feedback in the control systems [30, 31].

Before giving the main results, we recalled some lemmas which will be utilized in the subsequent control development and analysis.

Lemma 7 (Kalman-Yakubovich-Popov Lemma, [32]). *Let $G(s) = C(sI - A)^{-1}B + D$ be transfer function matrix where (A, B) is controllable and (A, C) is observable. Then, $G(s)$ is strictly positive real (SPR) if and only if there exist matrices $P = P^T > 0, Q = Q^T > 0$ such that*

$$PA + A^T P = -Q$$
$$B^T P = C \tag{4}$$

Lemma 8 (certainty equivalence stabilization, [33]). *For every fixed $\sigma = \chi(p)$, the switched system is detectable with respect to its equilibrium input-output pairs if (i) the process model is detectable about each of its equilibrium input-output pairs and (ii) the injected system is input-to-state stable with respect to its input.*

Lemma 9 (scale-independent hysteresis switching, [34]). *Let $N_\sigma(t, t_0)$ be the number of discontinuities of σ, which is generated by hysteresis switching logic, in the open interval (t_0, t). Let P be a finite set with m elements. For any $p \in P$ we have that*

$$N_\sigma(t, t_0) \le 1 + m + \frac{m}{\log(1+h)} \log\left[\frac{\pi_p(t)}{\min_{p\in P}\pi_p(t_0)}\right] \tag{5}$$

$$\int_{t_0}^{t} \dot{\pi}_\sigma(\tau)\, d\tau \le m\left[(1+h)\,\pi_p(t) - \min_{p\in P}\pi_p(t_0)\right] \tag{6}$$

3. Main Results

Based on the supervisory control system theory, in this paper, we design a multiestimator that meets M.P to cover all possible actuator failure modes, a candidate controller for each estimator to make the fixed switched system satisfy D.P, and a nonlinear estimation error operator for different sensor faults such that the switching signal satisfies S.P and N.P.

3.1. Multiestimator for DPS with Actuator Failure. By augmenting a new state and utilizing acceleration feedback technology, the extended state observer proposed in this paper based on (3) will improve disturbance attenuation performance compared to the traditional one [9, 35]. The observer is designed as follows:

$$\begin{aligned}
\dot{\hat{\xi}} &= A_w\hat{\xi} + K_{y1}\tilde{y} + K_{\rho 1}\tilde{\rho} + K_{\nu 1}J(\psi)\dot{\tilde{\nu}}\\
\dot{\hat{\eta}} &= J(\psi)\hat{\nu} + K_{y2}\tilde{y} + K_{\rho 2}\tilde{\rho} + K_{\nu 2}J(\psi)\dot{\tilde{\nu}}\\
\dot{\hat{b}} &= -A_b^{-1}\hat{b} + K_{y3}\tilde{y} + K_{\rho 3}\tilde{\rho} + K_{\nu 3}J(\psi)\dot{\tilde{\nu}}\\
\dot{\tilde{\rho}} &= K_{y4}\tilde{y} + K_{\rho 4}\tilde{\rho} + K_{\nu 4}J(\psi)\dot{\tilde{\nu}}\\
M\dot{\hat{\nu}} &= TKT_p + J^T(\psi)\hat{b} - D\hat{\nu} + J^T(\psi)K_{y5}\tilde{y}\\
&\quad + J^T(\psi)K_{\rho 5}\tilde{\rho} + K_{\nu 5}\dot{\tilde{\nu}}
\end{aligned} \tag{7}$$

where $\hat{\xi} \in \mathbb{R}^6, \hat{b} \in \mathbb{R}^3, \hat{\eta} \in \mathbb{R}^3, \hat{\nu} \in \mathbb{R}^3$ are the state vectors of observer, $\tilde{\rho} \in \mathbb{R}^3$ is a new extended state, $\tilde{y} = y - \hat{y}$ is the estimation error of position, $\dot{\tilde{\nu}} = \dot{\nu} - \dot{\hat{\nu}}$ is acceleration estimation error, and $K_{yi}, K_{\rho i}$, and $K_{\nu i}, i \in \{1, \ldots, 5\}$ are observer gain matrices with an appropriate dimension. Note that, for different thruster failures, the value of the matrix K will be different.

The acceleration feedback control law is designed as $T_p = (TK)^+(TK\overline{T}_p - K_{\nu 5}\dot{\nu})$, where $\overline{T}_p$ is called virtual control law and $K_{\nu 5}$ is the designed matrix such that the new inertia matrix $M_K = M + K_{\nu 5}$ is a positive definite diagonal matrix. Then the velocity dynamics of ship and observer can be rewritten as

$$\begin{aligned}
M_K\dot{\nu} &= TK\overline{T}_p + J^Tb - D\nu\\
M_K\dot{\hat{\nu}} &= TK\overline{T}_p + J^T\hat{b} - D\hat{\nu} + J^TK_{y5}\tilde{y} + J^TK_{\rho 5}\tilde{\rho}
\end{aligned} \tag{8}$$

Then acceleration estimation error equation can be rewritten as

$$M_K\dot{\tilde{\nu}} = J^T\tilde{b} - D\tilde{\nu} - J^TK_{y5}\tilde{y} - J^TK_{\rho 5}\tilde{\rho} \tag{9}$$

Now, we can deduce the error dynamics equation according to Assumption 3:

$$\begin{aligned}
\dot{\tilde{\xi}} &= (A_w + L_{11}C_w)\tilde{\xi} + L_{11}\tilde{\eta} + L_{12}\tilde{\rho} - L_{13}\tilde{b}\\
&\quad + K_{\nu 1}JM_K^{-1}D\tilde{\nu}\\
\dot{\tilde{\eta}} &= L_{21}C_w\tilde{\xi} + L_{21}\tilde{\eta} + L_{22}\tilde{\rho} - L_{23}\tilde{b}\\
&\quad + \left(K_{\nu 2}JM_K^{-1}D + J\right)\tilde{\nu}\\
\dot{\tilde{b}} &= L_{31}C_w\tilde{\xi} + L_{31}\tilde{\eta} + L_{32}\tilde{\rho} - \left(L_{33} + A_b^{-1}\right)\tilde{b}\\
&\quad + K_{\nu 3}JM_K^{-1}D\tilde{\nu}\\
\dot{\tilde{\rho}} &= -L_{41}C_w\tilde{\xi} - L_{41}\tilde{\eta} - L_{42}\tilde{\rho} + L_{43}\tilde{b} - K_{\nu 4}JM_K^{-1}D\tilde{\nu}
\end{aligned} \tag{10}$$

where $L_{i1} = K_{\nu i}M_K^{-1}K_{y5} - K_{yi}, L_{i2} = K_{\nu i}M_K^{-1}K_{\rho 5} - K_{\rho i}, L_{i3} = K_{\nu i}M_K^{-1}$. Since $\|J(\psi)\|_2 = \sqrt{3}$, the parameters can always be selected to make $\|K_{\nu 2}JM_K^{-1}D\|_2 >> \|J(\psi)\|_2$. Let $\tilde{x} = [\tilde{\xi}^T, \tilde{\eta}^T, \tilde{b}^T, \tilde{\rho}^T]^T$, and then the error dynamics equation can be written in compact form as follows:

$$\dot{\tilde{x}} = A\tilde{x} + BJ(\psi)D\tilde{\nu} \tag{11}$$

$$M_K\dot{\tilde{\nu}} = -D\tilde{\nu} - J^T(\psi)C\tilde{x} \tag{12}$$

where

$$\begin{aligned}
A &= \begin{bmatrix} A_w + L_{11}C_w & L_{11} & -L_{13} & L_{12}\\ L_{21}C_w & L_{21} & -L_{23} & L_{22}\\ L_{31}C_w & L_{31} & -\left(L_{33} + A_b^{-1}\right) & L_{32}\\ -L_{41}C_w & -L_{41} & L_{43} & -L_{42} \end{bmatrix}\\
B &= \begin{bmatrix} K_{\nu 1}M_K^{-1}\\ K_{\nu 2}M_K^{-1}\\ K_{\nu 3}M_K^{-1}\\ -K_{\nu 4}M_K^{-1} \end{bmatrix}\\
C &= \begin{bmatrix} K_{y5}C_w & K_{y5} & -I & K_{\rho 5} \end{bmatrix}
\end{aligned} \tag{13}$$

Theorem 10. *Considering the dynamic positioning vessel defined by (3) under Assumptions 1, 3, 5, the proposed observer given by (7) ensures the exponential convergence of the tracking errors; i.e., the multiestimator given by (7) satisfies M.P.*

Proof. By defining a new variable $\tilde{z} = C\tilde{x}$, the error dynamics can be rewritten as

$$\begin{aligned}
\dot{x} &= Ax + BJ(\psi)D\tilde{\nu}\\
\tilde{z} &= C\tilde{x}\\
\dot{\tilde{\nu}} &= -M_KD\tilde{\nu} - M_KJ^T(\psi)\tilde{z}
\end{aligned} \tag{14}$$

Since each element of system matrix A, B, and C contains a gain matrix to be designed, it is always possible to design system (14) to satisfy Lemma 7. In addition, as mentioned in [18], given a set of observer gains, the existence of the system to satisfy Lemma 7 can be checked numerically by using the Frequency Theorem.

Consider the following Lyapunov function candidate:

$$V = \tilde{\nu}^T D^T M_K \tilde{\nu} + \tilde{x}^T P \tilde{x} \tag{15}$$

If we choose the acceleration feedback to make M_K and D commutative, then we have $D^T M_K > 0$ according to Assumption 1.

The time differentiation of V along the trajectories of $\tilde{\nu}$ and $\tilde{x}$, according to Lemma 7, yields

$$\begin{aligned}
\dot{V} &= \dot{\tilde{\nu}}^T D^T M_K D^{-1} D\tilde{\nu} + (D\tilde{\nu})^T M_K D^{-1} D\dot{\tilde{\nu}} + 2\tilde{x}^T P\dot{\tilde{x}} \\
&= \left(-M_K^{-1} D\tilde{\nu} - M_K^{-1} J^T C\tilde{x}\right)^T D^T M_K D^{-1} D\tilde{\nu} \\
&\quad + (D\tilde{\nu})^T M_K D^{-1} D\left(-M_K^{-1} D\tilde{\nu} - M_K^{-1} J^T C\tilde{x}\right) \\
&\quad + \tilde{x}^T \left(PA + A^T P\right)\tilde{x} + 2\tilde{x}^T PBJD\tilde{\nu} \\
&= -(D\tilde{\nu})^T M_K^{-1} D M_K D^{-1} D\tilde{\nu} \\
&\quad - (D\tilde{\nu})^T \left(D^{-1} M_K D M_K^{-1} + M_K D^{-1} D M_K^{-1}\right) J^T C\tilde{x} \\
&\quad - (D\tilde{\nu})^T D\tilde{\nu} - \tilde{x}^T Q\tilde{x} + 2(D\tilde{\nu})^T J^T B^T P\tilde{x} \\
&= -2(D\tilde{\nu})^T D\tilde{\nu} - 2(D\tilde{\nu})^T J^T \left(C - B^T P\right)\tilde{x} - \tilde{x}^T Q\tilde{x} \\
&= -2\tilde{\nu}^T D^T D\tilde{\nu} - \tilde{x}^T Q\tilde{x} \le -\frac{\lambda_1}{\lambda_2} V
\end{aligned} \tag{16}$$

where $\lambda_1 \triangleq \min\{\lambda_{\min}(2D^T D), \lambda_{\min}(Q)\}$, and $\lambda_2 \triangleq \max\{\lambda_{\max}(D^T M_K), \lambda_{\max}(P)\}$.

In conclusion, we prove that the estimation error is exponentially convergent. Then there must exists at least one particular $[\hat{\xi}, \hat{\eta}, \hat{b}, \hat{\nu}]$ to provide a good approximation of the output $[\xi, \eta, b, \nu]$ for any actuator failure $K_p \in \mathfrak{K}$. □

3.2. Candidate Virtual Controller. In this subsection, a candidate controller is designed to make the injected system, consisting of observer (7) and candidate controller itself, input-to-state stable and ensure the switched system satisfies D.P.

By defining $y = \hat{y} - e_y$, $J(\psi)\dot{\nu} = J(\psi)\dot{\hat{\nu}} - e_\nu$, and designing an acceleration feedback control law $T_p = (TK)^+(TK\overline{T}_p - K_{\nu 5}\dot{\nu})$, where $\overline{T}_p$ is virtual control law to be designed, we can transform the observer equation (7) into the following injected form:

$$\dot{x}_E = A_E(\psi)\, x_E - B_E(\psi)\, e + B_u \overline{T}_p \tag{17}$$

where $x_E = [\hat{\xi}, \hat{\eta}, \hat{b}, \tilde{\rho}, \hat{\nu}]^T$, $e = [e_y, e_\nu]^T$.

$$A_E = \begin{bmatrix} A_w & 0 & 0 & K_{\rho 1} & 0 \\ 0 & 0 & 0 & K_{\rho 2} & J \\ 0 & 0 & -A_b^{-1} & K_{\rho 3} & 0 \\ 0 & 0 & 0 & K_{\rho 4} & 0 \\ 0 & 0 & M_K^{-1} J^T & M_K^{-1} J^T K_{\rho 5} & -M_K^{-1} D \end{bmatrix}$$

$$B_E = \begin{bmatrix} K_{y1} & K_{\nu 1} \\ K_{y2} & K_{\nu 2} \\ K_{y3} & K_{\nu 3} \\ K_{y4} & K_{\nu 4} \\ M_K^{-1} J^T K_{y5} & 0 \end{bmatrix}, \tag{18}$$

$$B_u = \begin{bmatrix} O_{6\times 1} \\ O_{3\times 1} \\ O_{3\times 1} \\ O_{3\times 1} \\ M_K^{-1} TK \end{bmatrix}$$

Note that the inertia of vessel is very large and the acceleration can be omitted; hence it is reasonable to select acceleration as the input of the injected system. Now we need to design control law to make the injected system (17) input-to-state stable with respect to the input e. Note that the state x_E is available for control, which is reasonable because multiestimator is implemented by the controller designer. Then we choose the virtual control law as follows:

$$\begin{aligned}
\overline{T}_p &= \left(M_K^{-1} TK\right)^+ \left(U_\xi \operatorname{diag}\left(J^T, J^T\right)\hat{\xi} + U_\eta J^T \hat{\eta}\right. \\
&\quad + \left(U_b - M_K^{-1}\right) J^T \hat{b} + \left(U_\rho J^T - M_K^{-1} J^T K_{\rho 5}\right)\tilde{\rho} \\
&\quad \left. + \left(M_K^{-1} D + U_\nu\right)\hat{\nu} + M_K^{-1} J^T K_{y5}\left(\hat{y} - y\right)\right)
\end{aligned} \tag{19}$$

Theorem 11. *Consider the injected system consisting of observer (7) and candidate controller $T_p = (TK)^+(TK\overline{T}_p - K_{\nu 5}\dot{\nu})$, where $\overline{T}_p$ is chosen as (19). The switched system, which contains injected system and plant, will satisfy D.P.*

Proof. When the observer gain matrices are selected as the following form: $k_{p1} = \operatorname{diag}(\operatorname{diag}(a, a, b), \operatorname{diag}(c, c, d))$, $K_{pi} = \operatorname{diag}(e, e, f)(i \in 2, 3, 4)$, one assumed that the bias time constants A_b has the same form, and wave peak frequency ω_{0i} in surge and sway are the same, so does relative damping ratio ζ_i. Then replace the virtual control law into the orginal injected system (17), and we have

$$\dot{x}_E = W^T(\psi)\,\overline{A} W(\psi)\, x_E - \overline{B}(\psi)\, e \tag{20}$$

where $W(\psi) = \mathrm{diag}(J^T(\psi), \ldots, J^T(\psi), I_{3\times 3})$,

$$\overline{A} = \begin{bmatrix} A_w & 0 & 0 & K_{\rho 1} & 0 \\ 0 & 0 & 0 & K_{\rho 2} & I \\ 0 & 0 & -A_b^{-1} & K_{\rho 3} & 0 \\ 0 & 0 & 0 & K_{\rho 4} & 0 \\ U_\xi & U_\eta & U_b & U_\rho & U_v \end{bmatrix},$$
$$\overline{B} = \begin{bmatrix} K_{y1} & K_{v1} \\ K_{y2} & K_{v2} \\ K_{y3} & K_{v3} \\ K_{y4} & K_{v4} \\ 0 & 0 \end{bmatrix} \tag{21}$$

The control gains and observer gains which appear in $\overline{A}$ are chosen such that the matrix $\overline{A}$ is asymptotically stable. Then there exists a matrix $P = P^T > 0$ such that $P\overline{A} + \overline{A}^T P = -Q$ for a given matrix $Q = Q^T > 0$. Besides, it should be noted that the injected system (20) is input-to-state stable if the system $\dot{z} = W^T(\psi)\overline{A}W(\psi)z$ is asymptotically stable [27]. Differentiate $W(\psi)z$ along the trajectories z, and we have

$$\frac{d\left(W\left(\psi\right)z\right)}{dt} = \dot{\psi}\overline{S}W\left(\psi\right)z + \overline{A}W\left(\psi\right)z \tag{22}$$

where $\overline{S} = \mathrm{diag}(S^T, \ldots, S^T, 0)$,

$$S = \begin{bmatrix} 0 & -1 & 0 \\ 1 & 0 & 0 \\ 0 & 0 & 0 \end{bmatrix} \tag{23}$$

Consider a Lyapunov function candiate

$$V\left(z\right) = z^T W^T\left(\psi\right) PW\left(\psi\right) z \tag{24}$$

Differentiate it:

$$\begin{aligned} \frac{dV}{dt} &= \left[\left(\dot{\psi}\overline{S} + \overline{A}\right)W\left(\psi\right)z\right]^T PW\left(\psi\right)z + \left(W\left(\psi\right)z\right)^T \\ &\cdot P\left[\left(\dot{\psi}\overline{S} + \overline{A}\right)W\left(\psi\right)z\right]^T = \left(W\left(\psi\right)z\right)^T \\ &\cdot \left[\left(\overline{A}^T + \dot{\psi}\overline{S}^T\right)P + P\left(\dot{\psi}\overline{S} + \overline{A}\right)\right]W\left(\psi\right)z \\ &= \left(W\left(\psi\right)z\right)^T\left[-Q + r\overline{S}^T P + rP\overline{S}\right]W\left(\psi\right)z \\ &\leq \left[-\lambda_{\min}\left(Q\right) + 2r_{\max}\lambda_{\max}\left(P\right)\right]\left\|W\left(\psi\right)z\right\|^2 \end{aligned} \tag{25}$$

When $r_{\max}$ is sufficiently small, the system $\dot{z} = W^T(\psi)\overline{A}W(\psi)z$ is asymptotically stable. Then the injected system (20) is input-to-state stable with respect to e.

Obviously, when there is no sensor failure, the dynamic positioning vessel satisfies detectability, which means that the state of plant eventually becomes small if the inputs and outputs are small. Then, according to Lemma 8, we can deduce that the switched system satisfies the D.P. □

3.3. NEEO for Different Sensor Failures. Sensor failures will damage the detectability of the vessel. In order to illustrate the problem, the following possible sensor failures are considered in this paper:

$$y = g \circ h\left(x\right) \tag{26}$$

where g, the sensor fault function, satisfies $g \circ h(0) \neq 0$; i.e., the detectability of plant is not satisfied. The detectability of switched system will not be guaranteed if we design supervisor in traditional way. One reason is that the measured output is no longer a true reflection of the actual value.

In this paper, a nonlinear estimation error operator (NEEO) is introduced to solve the above problems. Firstly, the process model (3) is remodeled as follows:

$$\begin{aligned} \dot{x} &= f\left(x, T_p\right) \\ y &= \begin{cases} y_n = h\left(p, x\right), & \text{no sensor failure} \\ y_f = g_j \circ h\left(p, x\right), & j^{th} \text{ sensor failure} \end{cases} \end{aligned} \tag{27}$$

where $x = [\xi^T, \eta^T, b^T, v^T]^T$. For convenience of analysis, suppose that $i \in P$, $j \in K$ which represents the different actuator failures and sensor failures, respectively. The multiestimator is designed for process (27):

$$\begin{aligned} \dot{x}_{Ei} &= F_i\left(x_{Ei}, T_p, y\right) \\ y_i &= h_i\left(x_{Ei}\right) \\ \dot{x}_{Ej} &= F_j\left(x_{Ej}, T_p, y\right) = F_i\left(x_{Ej}, T_p, g_j^{-1}\left(y\right)\right) \\ y_j &= h_i\left(x_{Ej}\right), \quad j = \#P \times k + i, i \in P \end{aligned} \tag{28}$$

where each $F_i, i \in P$, is the observer based on actuator failure just like Section 3.1.

Theorem 10 has proved that the estimator can track the true output $g_j^{-1}(y)$, so we define the nonlinear estimation error as $e_p = y_p \boxminus y$, where $\boxminus$ is NEEO, and the specific form is as follows:

$$e_p = y_p \boxminus y = \begin{cases} e_i = y_i - y, & i \in P \\ e_j = y_j - g_j^{-1}\left(y\right), & j \in K \end{cases} \tag{29}$$

No matter if the sensor is fault or not, there will always be a particular e_{p^*} that is convergent, which means the multiestimator satisfies M.P. Note that although the nonlinearity of e_p is caused by the existence of g, it does not affect the design of the front candidate controller (19). Moreover, sensor failures only change the controller's external input without any changing in the internal structure. Therefore, the following result is concluded.

Theorem 12. *Consider the dynamic positioning vessel described by (3) under Assumptions 1, 3, 5, the multiestimator given by (28) satisfies M.P, and the switched system also satisfies D.P.*

Remark 13. Obviously, to solve the problem of detectability loss caused by sensor faults, the fault information is needed, which can be achieved through fault reconstruction [36].

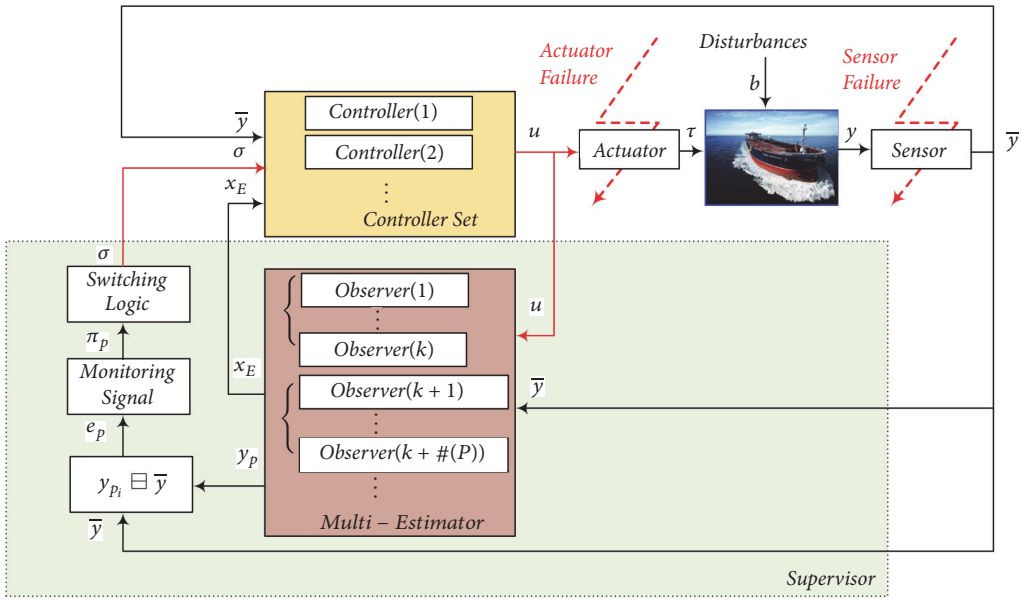

Figure 3: Fault-Tolerant Supervisory Control with NEEO for DPS.

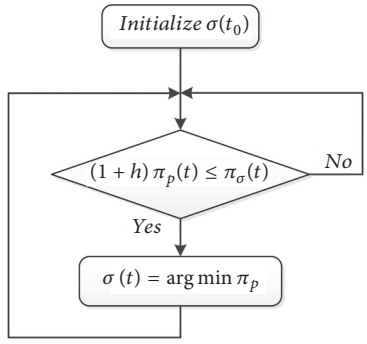

Figure 4: Scale-Independent Hysteresis Switching Logic.

3.4. Supervisory Control for Fault Tolerant. Taking into account the contents of all three previous parts, this section employs the scale-independent hysteresis switching logic to control the DPS with actuator failures and sensor failures. Figure 3 shows the structure of the proposed supervisory control system. The multiestimator comprises $(\#(P) \times \#(K))$ models, and the controller set comprises $\#(P)$ candidate controllers corresponding to the same $\#(P)$ actuator failures.

The hysteresis switching logic will be used to slow down switching based on the observed growth of the estimation errors [37]. Figure 4 shows the architecture of scale-independent hysteresis switching logic, where π_p physically is a monitoring signal in terms of the error norm as follows [22]:

$$\pi_p = \epsilon + e^{-\lambda t}\epsilon_0 + \int_0^t e^{-\lambda(t-\tau)}\overline{\gamma}\left(\left\|e_p(\tau)\right\|\right)d\tau \tag{30}$$

where ϵ, ϵ_0 are nonnegative constants of which at least one of them is strictly positive, and λ is a constant nonnegative forgetting factor, and $\overline{\gamma}$ is class K function.

Theorem 14. *Consider the dynamic positioning vessel (27), the multiestimator is designed as (28), the candidate acceleration feedback control law is designed as* $T_p = (TK)^{+}(TK\overline{T}_p - K_{v5}\dot{v})$ *with a virtual control law* $\overline{T}_p$ *(19), and the NEEO is chosen as (29). Then, under the supervisor with the scale-independent hysteresis switching logic, all states of the DPS are bounded no matter if the failures occur or not.*

Proof. The scaled version monitoring signal is defined as $\overline{\pi}_p(t) = \pi_p(t)e^{\lambda t}, \epsilon_0 = 0$. Based on Theorem 12, multiestimator satisfies M.P, so there exists $c_1 > 0$ such that $e_p^* < c_1$. Since the function $\overline{\gamma}$ is Lipschiz continuous, then

$$\begin{aligned}\overline{\pi}_p^*(t) &= \epsilon e^{\lambda t} + \int_0^t e^{\lambda s}\overline{\gamma}\left(\left\|e_p^*(s)\right\|\right)ds \\ &\le \epsilon e^{\lambda t} + \overline{\gamma}(c_1)\frac{1}{\lambda}e^{\lambda s}\Big|_0^t \le e^{\lambda t}\left[\epsilon + \frac{\overline{\gamma}(c_1)}{\lambda}\right] \\ &\le e^{\lambda t}c_2\end{aligned} \tag{31}$$

Using Lemma 9, we have

$$\begin{aligned}N_\sigma &\le m + \frac{m}{\ln(1+h)}\ln\left(\frac{\overline{\pi}_q(t)}{\min\overline{\pi}_p(t_0)}\right) \\ &\le m + \frac{m}{\ln(1+h)}\ln\left[\frac{c_2 e^{\lambda t}}{\epsilon e^{\lambda t_0}}\right] \\ &\le m + \frac{m}{\ln(1+h)}\ln\left(\frac{c_2}{\epsilon}\right) + \frac{t-t_0}{\ln(1+h)/\lambda m}\end{aligned} \tag{32}$$

$$\begin{aligned}&\int_0^t e^{\lambda s}\overline{\gamma}\left(\left|e_{\sigma(s)}(s)\right|\right)ds + \epsilon e^{\lambda t} - \epsilon \\ &\leq m\left[(1+h)\,\overline{\mu}_q(t) - \min\overline{\mu}_p(t_0)\right] \\ &\leq m(1+h)\,c_2 e^{\lambda t}\end{aligned} \tag{33}$$

Then we can choose $\ln(1+h)/\lambda m > \ln\mu/(\lambda_o - \lambda)$ such that the switching signal stasfities average dwell-time [38]. Since the choice of the virtual control law ensures the input-to-state stability of the injected system, then the state of switched injected system x_E has the property (Theorem 3.1,[25])

$$\begin{aligned}e^{\lambda t}\overline{\alpha}_1\left(\left\|x_E(t)\right\|\right) &\leq c\overline{\alpha}_2\left(\left\|x_E(0)\right\|\right) \\ &\quad + c\int_0^t e^{\lambda s}\overline{\gamma}\left(\left\|e_\sigma(s)\right\|\right)ds\end{aligned} \tag{34}$$

Substitute (33) into (34), and then

$$\left\|x_E(t)\right\| \leq \overline{\alpha}_1^{-1}\left(c\overline{\alpha}_2\left(\left\|x_E(0)\right\|\right) + cm(1+h)\,c_2\right) = c_3 \tag{35}$$

which means that the state of injected system is bounded. Then the output of injected system $y_p = h_p(x_E), (\forall p \in P)$ and switched thrust force T_{p_σ} are bounded too. Since $g^{-1}(y) = y_{p^*} - e_{p^*}$, then $\exists p^* \in P$, $g^{-1}(y)$ is bounded too. Then by the detectability of surface vessel with respect to the $g^{-1}(y)$, i.e. $h(0) = 0$, we can deduce that the state of plant is bounded. □

4. Simulation Research

A model of a DP vessel with 4 channel thrusters and 2 main thrusters is used in the simulation to demonstrate the performance of the supervisory control in case of actuator failures and sensor failures. For simplicity, we choose four types of actuator stuck failures $\mathfrak{K} \triangleq \{K_{f1}, K_{f2}, K_{f3}, K_{f4}\}$, where K_{f1}, K_{f2} denote the single actuator failure and K_{f3}, K_{f4} denote the multiple actuator failure. The simulation parameters are given in Table 1.

As shown in Table 2, only actuator failures are considered in Case 1 and Case 2, and both actuator failures and sensor failures are considered in Case 3. The expected position and heading vectors are taken as $\eta_d = [0m, 0m, 0rad]^T$ and the initial states are taken as $\eta(t_0) = [20m, 20m, 1rad]^T$. Simulation results of the proposed fault-tolerant control strategy are depicted in Figures 5–9.

It can be observed from Figure 5 that the acceleration estimation errors are very small enough to be ignored. So it is reasonable to take the acceleration estimation errors as an input of the injected system.

To illustrate the performance of the proposed control scheme, comparison results are presented by applying the FTC based on FDI in [5]. The initial states for both control schemes are chosen to be the same to guarantee a fair comparison. As shown in the detailed time responses of Figure 7, both methods can stabilize the vessel's state to the reference value with small bounded errors, but the method in [5] cannot deal with high frequency wave force very well, which is the weakness of the control based on low-frequency

Table 1: Main simulation parameters.

Symbol	Parameter values
M	$10^7 \times$ [3.64,0,0;0,4.35,2.49;0,2.49,7520.95]
D	$10^6 \times$ [3.22,0,0;0,3.22,-2.78;0,-2.78,815.06]
A_b	diag[1000,1000,1000]
B_b	diag[50000,56000,500000]
$A_w(21)$	diag[-0.81,-0.81,-0.81]
$A_w(22)$	diag[-0.18,-0.18,-0.18]
A_w	$[0_{3\times3}, I_{3\times3}; A_w(21), A_w(22)]$
B_w	$[[0_{3\times3}$; diag[16, 12, 0.25]]
K_{f1}	diag[0,1,1,1,1,1]
K_{f2}	diag[1,1,1,1,0,1]
K_{f3}	diag[0,1,1,0,1,0]
K_{f4}	diag[1,0,1,0,1,1]
g_1	$g_1(s,t) = 2s + 10\sin(t)$
T	[000011;111100;50.4,41.8,-35.7,-45,4.5,-4.5]

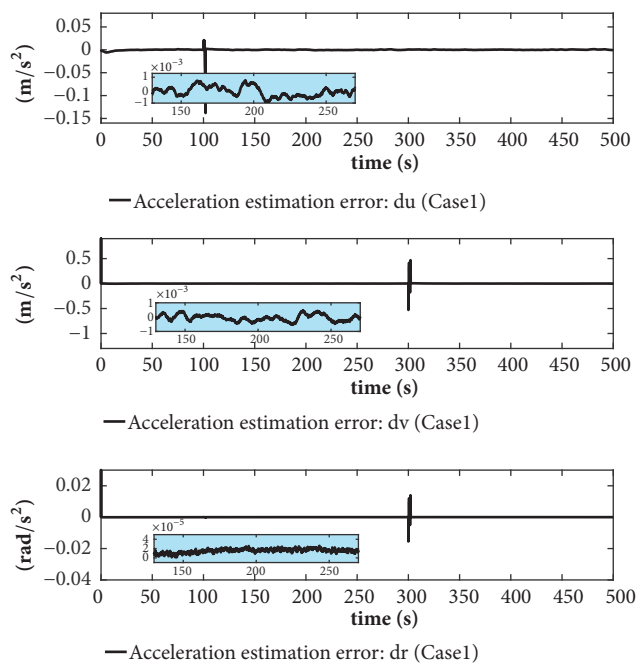

Figure 5: Acceleration Estimation Error.

model. Therefore, the proposed fault-tolerant control method is more effective for the dynamic positioning ships in the presence of high frequency wave disturbance.

Remark 15. The upper bound on the maximum number of simultaneously isolable actuator faults in [5] is determined by the Uniform Sub-Rank of the matrix, which is related to the control input matrix B and thruster matrix T. By calculation, we can deduce that the method in [5] can only solve the single actuator fault. So only Case 1 is considered in the comparison part.

Table 2: Condition of faults.

Time(s)	0-100	100-250	250-300	300-500
Case 1	$K = K_{f1}$	$K = K_{f2}$	$K = K_{f2}$	$K = K_{f1}$
Case 2	$K = K_{f3}$	$K = K_{f4}$	$K = K_{f4}$	$K = K_{f3}$
Case 3	$K = K_{f3}$	$K = K_{f4}$	$K = K_{f4}, g = g_1$	$K = K_{f3}, g = g_1$

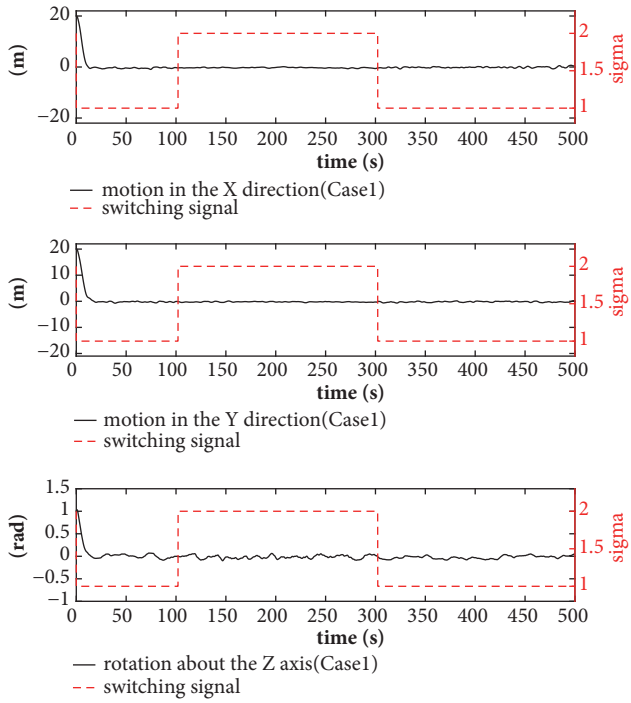

Figure 6: Position and Heading of DP Vessel (Case 1).

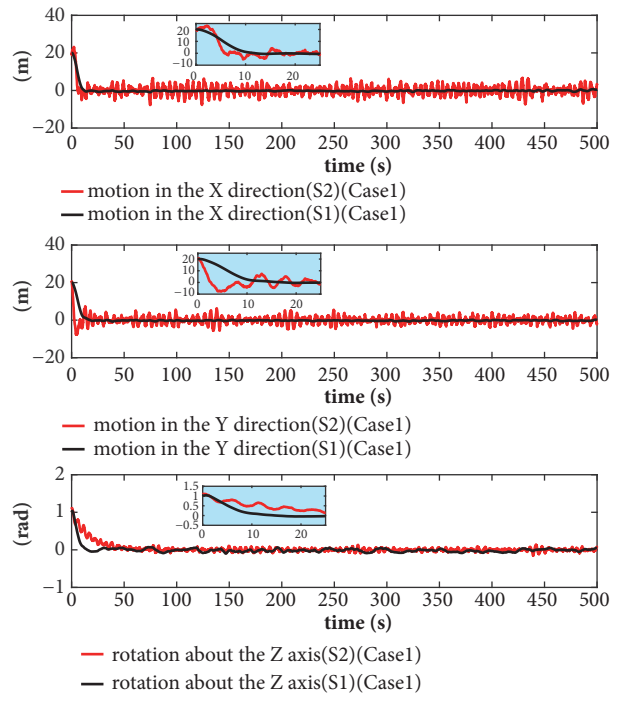

Figure 7: The tracking performance comparison of the proposed method (S1)(Case 1) and fault-tolerant control allocation [5] (S2)(Case 1).

Control performances of Case 2 and Case 3, where multiple actuator failures occur, are demonstrated in Figures 8 and 9, respectively. Firstly, it is shown that the signal σ can switch to the corresponding controller quickly and accurately in the presence of actuator failures. Secondly, when a sensor failure occurs at 250s, although there is a slight fluctuation in the transition progress, the signal σ can switch to the stable controller, and positions of the vessel are stabilized near the equilibrium point eventually.

5. Conclusion

This paper presented a fault-tolerant supervisory control method for dynamic positioning ships with wave-frequency model. The proposed fault-tolerant control method does not need the FDI mechanism due to the introduction of injected system and supervisor. It has been proved that, by introducing a nonlinear estimation error and virtual controller, the detectability property and matching property of the switched system are guaranteed in the presence of actuator failures and sensor failures. Simulation results and comparisons have demonstrated the effectiveness of the proposed fault-tolerant control scheme. In the future, we will consider the unknown faults, which is more practical in realistic situation. Further, we will improve the switching logic to make the switching signal more accurate and stable for more serious failure.

Data Availability

All the data supporting the conclusions of the study have been provided in Simulation and readers can access these data in [27, 29].

Conflicts of Interest

The authors declare that there are no conflicts of interest related to this paper.

Acknowledgments

This research was partially supported by the National Science Technology Support Program of China (Project no. 51609046).

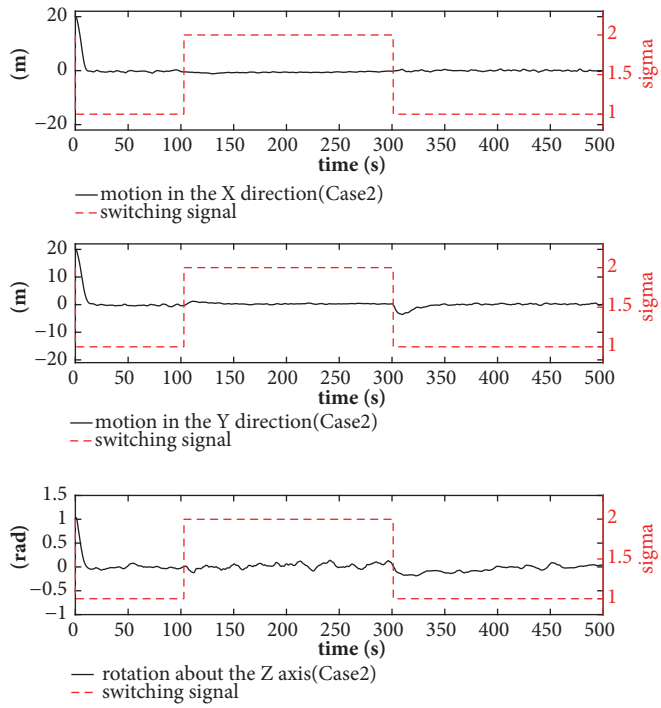

Figure 8: Position and Heading of DP Vessel (Case 2).

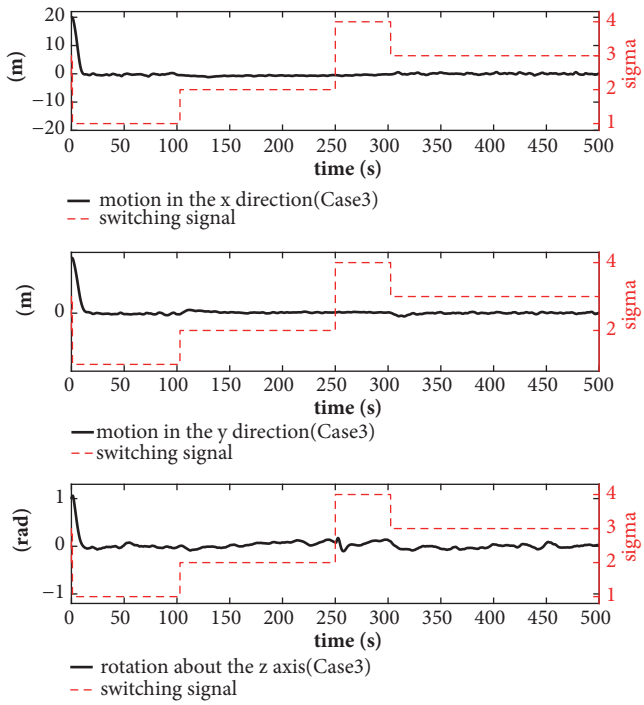

Figure 9: Position and Heading of DP Vessel (Case 3).

References

[1] H. Azmi and M. J. Khosrowjerdi, "Robust adaptive fault tolerant control for a class of Lipschitz nonlinear systems with actuator failure and disturbances," *Proceedings of the Institution of Mechanical Engineers, Part I: Journal of Systems and Control Engineering*, vol. 230, no. 1, pp. 13–22, 2016.

[2] S. Dai L and J. Zhao, "Reliable H8 controller design for a class of uncertain linear systems with actuator failures," *International Journal of Control Automation & Systems*, vol. 6, no. 6, pp. 954–959, 2008.

[3] Y. L. Hao and G. H. Yang, "Robust fault tolerant control based on sliding mode method for uncertain linear systems with quantization," *Proceedings of the Institution of Mechanical Engineers Part I Journal of Systems & Control Engineering*, vol. 52, no. 5, pp. 692–703, 2013.

[4] Z. Zuo, D. W. C. Ho, and Y. Wang, "Fault tolerant control for singular systems with actuator saturation and nonlinear perturbation," *Automatica*, vol. 46, no. 3, pp. 569–576, 2010.

[5] A. Cristofaro and T. A. Johansen, "Fault tolerant control allocation using unknown input observers," *Automatica*, vol. 50, no. 7, pp. 1891–1897, 2014.

[6] T. I. Fossen, *Handbook of Marine Craft Hydrodynamics and Motion Control*, 2011.

[7] A. J. Sørensen, "A survey of dynamic positioning control systems," *Annual Reviews in Control*, vol. 35, no. 1, pp. 123–136, 2011.

[8] J. Liu, R. Allen, and H. Yi, "Ship motion stabilizing control using a combination of model predictive control and an adaptive input disturbance predictor," *Proceedings of the Institution of Mechanical Engineers, Part I: Journal of Systems and Control Engineering*, vol. 225, no. 5, pp. 591–602, 2011.

[9] M. Tomera, "Nonlinear observers design for multivariable ship motion control," *Polish Maritime Research*, vol. 19, pp. 50–56, 2012.

[10] A. Hajivand and S. H. Mousavizadegan, "The effect of memory in observer design for a dp system," in *Proceedings of the ASME 2010 International Mechanical Engineering Congress and Exposition, IMECE 2010*, pp. 53–59, Canada, November 2010.

[11] M. Fu, J. Ning, and Y. Wei, "Fault-tolerant control of dynamic positioning vessel after thruster failures using disturbance

decoupling methods," in *Proceedings of the 2011 IEEE International Conference on Automation and Logistics, ICAL 2011*, pp. 433–437, China, August 2011.

[12] F. Benetazzo, G. Ippoliti, S. Longhi, and P. Raspa, "Advanced control for fault-tolerant dynamic positioning of an offshore supply vessel," *Ocean Engineering*, vol. 106, pp. 472–484, 2015.

[13] Y. Lin and J. Du, "Fault-tolerant control for dynamic positioning of ships based on an iterative learning observer," in *Proceedings of the 35th Chinese Control Conference, CCC 2016*, pp. 1116–1122, China, July 2016.

[14] M. Chen, B. Jiang, and R. Cui, "Actuator fault-tolerant control of ocean surface vessels with input saturation," *International Journal of Robust & Nonlinear Control*, vol. 26, no. 3, pp. 542–564, 2016.

[15] Y. Su, C. Zheng, and P. Mercorelli, "Nonlinear PD Fault-Tolerant Control for Dynamic Positioning of Ships With Actuator Constraints," *IEEE/ASME Transactions on Mechatronics*, vol. 22, no. 3, pp. 1132–1142, 2017.

[16] W.-Z. Yu, H.-X. Xu, and H. Feng, "Robust adaptive fault-tolerant control of dynamic positioning vessel with position reference system faults using backstepping design," *International Journal of Robust and Nonlinear Control*, vol. 28, no. 2, pp. 403–415, 2018.

[17] N. T. Dong, *Design of hybrid marine control systems for dynamic positioning [PhD thesis]*, 2006.

[18] J. P. Strand and T. I. Fossen, "Nonlinear passive observer design for ships with adaptive wave filtering," in *New Directions in Nonlinear Observer Design*, vol. 244 of *Lecture Notes in Control and Information Sciences*, pp. 113–134, Springer, London, UK, 1999.

[19] S. Saelid, J. G. Balchen, and N. A. Jenssen, "Design and analysis of a dynamic positioning system based on kalman filtering and optimal control," *IEEE Transactions on Automatic Control*, vol. 28, no. 3, pp. 331–339, 1983.

[20] G. Battistelli, J. P. Hespanha, and P. Tesi, "Supervisory control of switched nonlinear systems," *International Journal of Adaptive Control and Signal Processing*, vol. 26, no. 8, pp. 723–738, 2012.

[21] I. R. Bertaska and K. D. Von Ellenrieder, "Supervisory switching control of an unmanned surface vehicle," in *Proceedings of the MTS/IEEE Washington, OCEANS 2015*, USA, October 2015.

[22] J. P. Hespanha, "Tutorial on supervisory control," *Overview*, 2002.

[23] J. P. Hespanha, D. Liberzon, and A. S. Morse, "Supervision of integral-input-to-state stabilizing controllers," *Automatica*, vol. 38, no. 8, pp. 1327–1335, 2002.

[24] M. Skogvold, *Supervisory-switched control for dynamic positioning systems in arctic areas [Msc thesis]*, Department of Marine Technology, 2010.

[25] L. Vu, D. Chatterjee, and D. Liberzon, "Input-to-state stability of switched systems and switching adaptive control," *Automatica*, vol. 43, no. 4, pp. 639–646, 2007.

[26] E. D. Sontag, "Input to state stability: basic concepts and results," in *Nonlinear and Optimal Control Theory*, pp. 163–220, Springer, Heidelberg, Berlin, Germany, 2008.

[27] T. D. Nguyen, A. J. Sørensen, and S. T. Quek, "Design of hybrid controller for dynamic positioning from calm to extreme sea conditions," *Automatica*, vol. 43, no. 5, pp. 768–785, 2007.

[28] T. I. Fossen, "Marine Control Systems: Guidance, Navigation, and Control of Ships, Rigs and Underwater Vehicles," 2002.

[29] T. I. Fossen and J. P. Strand, "Passive nonlinear observer design for ships using Lyapunov methods: full-scale experiments with a supply vessel," *Automatica*, vol. 35, no. 1, pp. 3–16, 1999.

[30] G. Xia, X. Shao, H. Wang et al., "Passive nonlinear observer design for special structure vessels," *Oceans. IEEE*, pp. 1–8, 2013.

[31] K. P. Lindegaard, *Acceleration Feedback in Dynamic Positioning*, Fakultet for Informasjonsteknologi Matematikk Og Elektroteknikk, 2012.

[32] H. K. Khalil, *Nonlinear Systems*, Prentice-Hall, Upper Saddle River, NJ, USA, 3rd edition, 2002.

[33] J. P. Hespanha and A. S. Morse, "Certainty equivalence implies detectability," *Systems & Control Letters*, vol. 36, no. 1, pp. 1–13, 1999.

[34] J. P. Hespanha, D. Liberzon, and A. S. Morse, "Bounds on the number of switchings with scale-independent hysteresis: Applications to supervisory control," *Proceedings of the IEEE Conference on Decision and Control*, vol. 4, pp. 3622–3627, 2000.

[35] M. H. Kim and D. J. Inman, "Development of a robust nonlinear observer for dynamic positioning of ships," *Proceedings of the Institution of Mechanical Engineers Part I Journal of Systems & Control Engineering*, vol. 218, no. 1, pp. 1–11, 2004.

[36] H. Alwi, C. Edwards, and C. P. Tan, *Fault Detection and Fault-Tolerant Control Using Sliding Modes*, Advances in Industrial Control, Springer, London, UK, 2011.

[37] J. P. Hespanha, D. Liberzon, and A. S. Morse, "Hysteresis-based switching algorithms for supervisory control of uncertain systems," *Automatica*, vol. 39, no. 2, pp. 263–272, 2003.

[38] J. P. Hespanha and A. S. Morse, "Stability of switched systems with average dwell-time," in *Proceedings of the 38th IEEE Conference on Decision and Control (CDC '99)*, pp. 2655–2660, Phoenix, Ariz, USA, December 1999.